Earth Rotation-Aware Non-Stationary Satellite Communication Systems: Modeling and Analysis

Jia Ye, *Student Member, IEEE*, Gaofeng Pan, *Senior Member, IEEE*, and Mohamed-Slim Alouini, *Fellow, IEEE*

***Abstract*— In this paper, we propose a non-stationary satellite communication system model considering the impacts of Earth rotation by adopting the Earth-centered inertial (ECI), and the Earth-centered Earth-fixed (ECEF) coordinates. The position variations of a satellite (S) and a ground user (U) via coordinate transformations are demonstrated. Considering the variations of the distance between S and U, the instantaneous outage probability (OP) and channel capacity are calculated, as well as the system throughput within finite communication time. A simplified case is considered and analyzed while ignoring the Earth's rotation. Furthermore, the asymptotic expressions for the OP, capacity, and throughput are developed in the high signal-to-noise ratio (SNR) regime to obtain some insights. We also provide new definitions for throughput and OP within a short communication duration. The application and future research directions based on the derived results, including resource allocation, satellite handover, communication scenarios with multiple satellites and mobile users, are also discussed. Finally, some selected numerical results are provided to validate our proposed analysis models.**

***Index Terms*— Coordinate transformation, Earth-centered Earth-fixed coordinate, Earth-centered inertial coordinate, instantaneous capacity, instantaneous outage probability, throughput.**

I. Introduction

SATELLITE communications are becoming a necessary trend in 5G and beyond technologies [1]–[4] to support the exponentially increasing data transmissions and amount of online users across the world after it has been widely applied in mass broadcasting, navigation, and disaster relief operations for its capability of seamless connectivity, high data rate, and worldwide coverage [5].

As a promising strategy, satellite communication has attracted a significant amount of researchers to study its system performance, such as outage probability (OP) [6]–[9] and ergodic capacity [8], [10]–[13]. Most works considered complicated satellite-to-terrestrial-destination systems, in which the transmission between satellites and ground users is assisted by ground relays. For instance, the authors of [6] analyzed the OP of the transmission from the satellite to ground users assisted by a ground relay under two proposed cache placement schemes. The authors of [7] studied the OP of a multi-antenna satellite to multiple ground destinations system assisted by multiple ground relays, while a max–max user-relay selection scheme was adopted. In [9], the outage performance of a multi-user threshold-based decode-and-forward (DF) satellite relaying network assisted by spot beam technology was investigated. Moreover, throughput or ergodic capacity is another important indicator of system performance. The authors of [10] derived the asymptotic throughput of a satellite communication system suffering hardware impairments, in which a ground relay could transmit signals to both the satellite and the mobile user. Considering the statistical delay quality-of-service and interference-power limitations imposed by terrestrial networks, the effective capacity of the satellite network was analyzed [11]. The authors of [12] investigated the ergodic capacity of non-orthogonal multiple access based uplink satellite communication networks while considering randomly located users, imperfect channel state information, and antenna-pointing error. Assuming a different amount of channel state knowledge at the transmitter but perfect receive-side information, the corresponding ergodic capacity was studied in [13].

Although recent works have made considerable contributions to modeling and analyzing various kinds of satellite communication networks, especially with the assistance of ground relays [7]–[9], the effects of the satellite's rotation on the system performance have not been well-investigated. Most literature also ignored the influence of the Earth's rotation which exists in reality. Both position variations of the satellite and ground terminals play a crucial role in realistic satellite communication networks, because of unavoidable performance variations and necessary handover actions caused

Manuscript received July 14, 2020; revised November 7, 2020 and February 17, 2021; accepted April 3, 2021. Date of publication April 13, 2021; date of current version September 10, 2021. This work was supported in part by the Office of Sponsored Research at KAUST and in part by the NSF of China under Grant 62171031. The associate editor coordinating the review of this article and approving it for publication was A. Liu. *(Corresponding author: Gaofeng Pan.)*

Jia Ye and Mohamed-Slim Alouini are with the Computer Electrical and Mathematical Sciences and Engineering (CEMSE) Division, Department of Electrical Engineering, King Abdullah University of Science and Technology (KAUST), Thuwal 23955-6900, Saudi Arabia (e-mail: jia.ye@kaust.edu.sa; slim.alouini@kaust.edu.sa).

Gaofeng Pan was with the Computer Electrical and Mathematical Sciences and Engineering (CEMSE) Division, Department of Electrical Engineering, King Abdullah University of Science and Technology (KAUST), Thuwal 23955-6900, Saudi Arabia. He is now with the School of Cyberspace Science and Technology, Beijing Institute of Technology, Beijing 100081, China (e-mail: gaofeng.pan.cn@ieee.org).

Color versions of one or more figures in this article are available at https://doi.org/10.1109/TWC.2021.3071377.

Digital Object Identifier 10.1109/TWC.2021.3071377

by a considerable communication distance variation. There are some works [14], [15] analyzing the performance of satellite communication systems while considering the satellite's rotation. More specifically, the authors in [14] proposed a multi-satellite interference model equipped with a multi-beam antenna and evaluated its co-channel interference. The authors in [15] evaluated both geometrical performance measures and co-channel interference levels of low Earth orbit (LEO), medium-altitude Earth orbit (MEO), and geostationary orbit (GEO) satellite constellations, and proposed several interference reduction techniques. Although the impact of the satellite's rotation has been considered in these works, they ignored the effects of the Earth's rotation. Moreover, they did not analyze the system performance in a closed-form. When taking both the satellite's and the Earth's rotations into consideration, researchers' eyes are mainly focused on satellite handover [16], global positioning system [17]–[19], and navigation performance evaluation [19], [20]. Few works have investigated the outage performance and system capacity while considering the satellite's and the Earth's movement, which motivates us to mitigate this gap.

To evaluate the performance of time-varying systems caused by the movement of satellites at various altitudes and Earth's rotation, in this paper we consider the coordinate transformation to the Earth-centered inertial (ECI)-frame and Earth-centered Earth-fixed (ECEF)-frame. The ECI frame is responsible for calculating the satellite's position and velocity, while the ECEF frame is similar to the ECI frame but rotates along with the Earth, hence, it is fixed to the Earth [21]. Both frames are widely used in the researches about navigation satellite systems [22], [23], but very few on satellite communications.

In this paper, we analyze the system performance of non-stationary satellite communication scenarios, while taking the Earth's and satellite's rotations into account. A more practical system model is provided, where the satellite could only serve users in the coverage area within finite time. By ignoring the Earth's rotation, we also propose some simplified results accordingly. Moreover, we derive some asymptotic results to achieve more insights. New definitions of the throughput and the OP with short transmission duration are also proposed.

The main contributions of this paper are summarized as follows:

1) We introduce the coordinate transformation to the ECI frame and ECEF frame to illustrate the variation of the distance between the satellite (S) and the ground user (U) on the Earth.

2) We study the instantaneous OP, instantaneous channel capacity, and throughput for non-stationary satellite communication systems while considering both the satellite's and the Earth's rotations.

3) We provide some simplified results by ignoring the Earth's rotation. The simplified throughput is shown to be an upper bound to the general case.

4) In the high signal-to-noise ratio (SNR) regime, the asymptotic instantaneous OP, instantaneous channel capacity, and throughput for both cases are derived.

5) The application of our derived results, such as the optimal power allocation and some research directions, has been discussed.

6) Considering the short communication duration caused by the Earth's rotation, the satellite rotation, the initial U, and satellite position, new definitions for throughput and OP are proposed.

The derived analytical models can be used for any scenario, thereby avoiding the need for extensive simulations.

The rest of this paper is organized as follows. In Section II and III, the coordinate transformation, system, and channel models are described, respectively. In Section IV, system performance for the general case considering the Earth's rotation and the simplified case ignoring the Earth's rotation is investigated. In Section V, some asymptotic results are derived. Applications and future research directions are proposed in Section VI. In Section VII, new definitions for throughput and OP are proposed. Finally, numerical results are presented and discussed in Section VIII, and the conclusion of some remarks is conducted in Section IX.

II. ECEF Satellite Coordinate Introduction

To demonstrate the effects of the rotations of the Earth and the satellite, we first introduce the ECI frame and the ECEF frame [21], [24]. Cartesian coordinates are commonly used to show the location of an object on the Earth by using the ECI. In ECI frame, the $x-y$ plane coincides with the equatorial plane of the Earth; the x-axis is permanently fixed in a direction relative to the celestial sphere, which does not rotate as the Earth does; and the z-axis lies at 90° to the equatorial plane and extends through the North Pole. Due to the forces that the sun and moon exert, the Earth's equatorial plane moves with respect to the celestial sphere. The Earth rotates, while ECI coordinate system does not. In contrast to the ECI frame, the ECEF frame is another coordinate that remains fixed concerning the Earth's surface in its rotation. This means that the ECEF frame rotates with the Earth, and therefore the coordinates of a point fixed on the surface of the Earth do not change.

As shown in Fig. 1, if we take the plane of the equator as the $x-y$ coordinate plane and the axis of the Earth's rotation tilted at an angle of 23.5° relative to the orbital plane as the z-axis, we could set up a spherical coordinate based on the Earth center, which is the ECI coordinate. Assuming the Earth rotates an angle of θ after a while, the new ECEF coordinate will be composed of x_T-axis, y_T-axis, and z-axis.

Assuming all satellite orbits take the Earth's core as the coordinate origin, all orbits could be obtained from a rotation of the satellite orbits set in the same plane as the equator. For example, one of the orbit coordinates could be obtained by rotating Ω degree about the z-axis and i degree about the x-axis in three dimensions by using the right-hand rule, as seen in Fig. 1. The obtained coordinate is composed of P-axis, Q-axis, and W-axis. However, to compute the distance between the satellites and users, we should put them in the same coordinates. To achieve this goal, we first re-express the

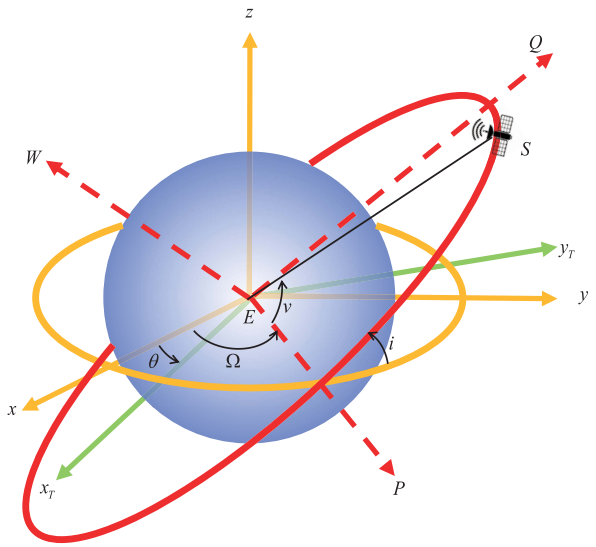

Fig. 1. Spherical coordinates.

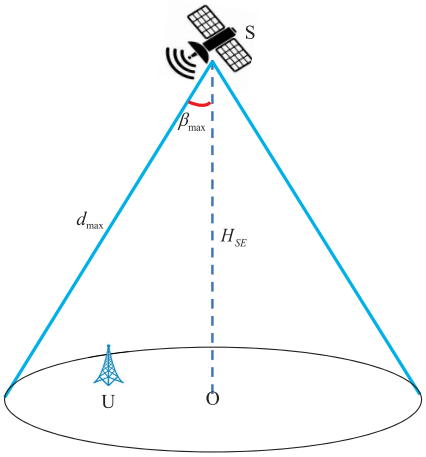

Fig. 2. Coverage area.

position of the satellite in ECI coordinate through coordinate transformation. Assuming there is a satellite with coordinate $\mathbf{s}_{0,S} = (H_S \cos(v), H_S \sin(v), 0)$, where v is the angle between the P-axis and the line ES, H_S is the height from S to the center of the Earth. The new coordinate of S on the ECI coordinate can be obtained by multiplying the unitary rotation matrices $\mathbf{R}_x(-i)$ and $\mathbf{R}_z(-\Omega)$, which can be expressed as

$$\mathbf{s}_{0,ECI} = \mathbf{R}_z(-\Omega)\mathbf{R}_x(-i)\mathbf{s}_{0,S}, \tag{1}$$

where $\mathbf{R}_x(\cdot)$ and $\mathbf{R}_z(\cdot)$ are the rotation matrices defined as

$$\mathbf{R}_x(\alpha) = \begin{bmatrix} 1 & 0 & 0 \\ 0 & \cos(\alpha) & -\sin(\alpha) \\ 0 & \sin(\alpha) & \cos(\alpha) \end{bmatrix} \tag{2}$$

and

$$\mathbf{R}_z(\alpha) = \begin{bmatrix} \cos(\alpha) & -\sin(\alpha) & 0 \\ \sin(\alpha) & \cos(\alpha) & 0 \\ 0 & 0 & 1 \end{bmatrix}. \tag{3}$$

Taking the rotation of the Earth into consideration, we should transform the coordinate in ECI coordinate further to ECEF coordinate. It means the coordinate of S in ECEF-coordinate with θ Earth's rotation is

$$\mathbf{s}_{ECEF} = \mathbf{R}_z(\theta)\mathbf{s}_{0,ECI}. \tag{4}$$

Assuming the coordinate of U is denoted as $\mathbf{u}_{ECEF}$, the distance between S and U can be calculated as

$$\begin{aligned} d_E &= \|\mathbf{s}_{ECEF} - \mathbf{u}_{ECEF}\|_2 \\ &= \|\mathbf{R}_z(\theta - \Omega)\mathbf{R}_x(-i)\mathbf{s}_{0,S} - \mathbf{u}_{ECEF}\|_2. \end{aligned} \tag{5}$$

III. System Model and Channel Model

In this section, we will introduce the considered non-stationary satellite communication system model as well as the channel model. Although we focus on the downlink transmission from a satellite to a ground user, the analysis can be extended to uplink transmissions in the same way. The ground user considered here can also be other kinds of ground terminals, like BS.

A. System Model

In a realistic satellite communication system, a satellite can only serve the terminals located in its coverage. A simplified coverage area of a satellite is presented in Fig. 2, where S only can serve U in the circle with maximal achievable angle $\beta_{\max}$ composed by the direct line from S to U, and the line from S to the center of the Earth. $\beta_{\max}$ depends on many aspects, such as hardware implementation, propagation environment, system design, and so on. The distance between S to the Earth surface H_{SE} and $\beta_{\max}$ decides the maximal communication distance, which can be calculated as

$$d_{\max} = \frac{H_{SE}}{\cos(\beta_{\max})}, \tag{6}$$

where $H_{SE} = H_S - H_E$, H_E is a fixed value that denotes the distance from the center of the Earth to the Earth's surface. It also denotes the distance between S and the edge of the coverage area. Assuming U locates in the coverage area of S, whose position could be denoted by

$$\begin{aligned} &\mathbf{u}_{ECEF} \\ &= [u_1, u_2, u_3]^T \\ &= [H_E \sin(\theta_u)\cos(\varphi_u), H_E \sin(\theta_u)\sin(\varphi_u), H_E \cos(\theta_u)]^T, \end{aligned} \tag{7}$$

where θ_u is the angle between the zenith direction and the line from the Earth's center to U, and φ_u is the signed angle measured from the azimuth reference direction to the orthogonal projection of the line segment from the Earth's center to U on the reference plane. It satisfies $\|\mathbf{u}_{ECEF}\|_2 = H_E$ in the ECEF coordinate. Since the Earth rotates 360 degrees every 24 hours, it rotates about $\omega_e = 0.0042$ degrees every second. Assuming that S rotates about ω_s degrees every second on its orbit, it is located at $\mathbf{s}_{0,S}$ when U falls into the coverage of S. Since the communication only starts when U falls into S's

coverage area, the initial distance between S and U can be denoted as

$$d_0 = \|\mathbf{s}_{0,ECEF} - \mathbf{u}_{ECEF}\|_2 = d_{\max}. \quad (8)$$

Considering the rotations of S and the Earth within rotation time t, the coordinate of U does not change in ECEF coordinate, while the position of S after t seconds in P-Q-W-axis is $\mathbf{s}_{t,S} = \mathbf{R}_z(\omega_s t)\mathbf{s}_{0,S}$. From P-Q-W-axis to ECEF coordinate, the position can be denoted as

$$\mathbf{s}_{t,ECEF} = \mathbf{R}_z(\omega_e t - \Omega)\mathbf{R}_x(-i)\mathbf{R}_z(\omega_s t)\mathbf{s}_{0,S}, \quad (9)$$

where $\mathbf{s}_{t,ECEF} = \begin{bmatrix} s_1 & s_2 & s_3 \end{bmatrix}^T$ can be separately calculated as

$$s_1 = \alpha_1 \cos(\omega_a t + \beta_1) + \alpha_2 \cos(\omega_m, t + \beta_2), \quad (10)$$

$$s_2 = \alpha_1 \sin(\omega_a t + \beta_1) + \alpha_2 \sin(\omega_m t + \beta_2), \quad (11)$$

and

$$s_3 = H_S \sin(-i) \sin(\omega_s t + v), \quad (12)$$

where $\alpha_1 = \frac{H_S}{2}[1 + \cos(i)]$, $\omega_a = \omega_e + \omega_s$, $\beta_1 = v - \Omega$, $\alpha_2 = \frac{H_S}{2}[1 - \cos(i)]$, $\omega_m = \omega_e - \omega_s$, $\beta_2 = -v - \Omega$.

Thus, the distance between U and S can be written as

$$\begin{aligned} d(t)^2 &= \|\mathbf{s}_{t,ECEF} - \mathbf{u}_{ECEF}\|_2^2 \\ &= \|\mathbf{R}_z(\omega_e t - \Omega)\mathbf{R}_x(-i)\mathbf{R}_z(\omega_s t)\mathbf{s}_{0,S} - \mathbf{u}_{ECEF}\|_2^2 \\ &= \|\mathbf{R}_z(\omega_e t - \Omega)\mathbf{R}_x(-i)\mathbf{R}_z(\omega_s t)\mathbf{s}_{0,S}\|_2^2 + \|\mathbf{u}_{ECEF}\|_2^2 \\ &\quad - 2\mathbf{u}_{ECEF}^T \mathbf{R}_z(\omega_e t - \Omega)\mathbf{R}_x(-i)\mathbf{R}_z(\omega_s t)\mathbf{s}_{0,S} \\ &= H_S^2 + H_E^2 - 2(u_1 s_1 + u_2 s_2 + u_3 s_3) \\ &= H + \mu_1 \cos(\omega_a t + \eta_1) \\ &\quad + \mu_2 \cos(\omega_m t + \eta_2) + \mu_3 \sin(\omega_s t + v), \end{aligned} \quad (13)$$

where $H = H_S^2 + H_E^2$, $\mu_1 = -2H_E \sin(\theta_u)\alpha_1$, $\mu_2 = -2\ H_E \sin(\theta_u)\alpha_2$, $\mu_3 = -2u_3 H_S \sin(-i)$, $\eta_1 = \beta_1 - \varphi_u$ and $\eta_2 = \beta_2 - \varphi_u$.

The communication time between S and U starts once U falls into the coverage area and ends when U is out of the coverage area of S, which is denoted as t_s and t_e, respectively. In the following, we denote the satellite visibility window as the period that starts when the ground terminal falls into the coverage area of the satellite and ends when the ground terminal is out of the coverage area of the satellite.

B. Channel Model

Similar to traditional terrestrial communications, the terrestrial propagation between the satellite and ground users can be divided into line-of-sight (LoS) case and non-LoS (NLoS) case, which depends on the location and environment of the ground user [25]. The LoS link is established when the connected ground terminal tends to be located in an open area without many objects surrounding it, while the NLoS link is established when the ground terminals are surrounded by objects, for example, the indoor terminals and terminals deployed in dense urban areas. Since satellite communications are expected to ensure service availability anywhere and to enable 5G network scalability by providing efficient multicast/broadcast resources for data delivery towards the network edges and user terminals, the system performance under both LoS and NLoS cases should be considered and investigated. In the following, we introduce the channel model, which is able to describe both NLoS and LoS propagation by setting appropriate parameters.

In mobile satellite communications, the channel is always modeled as a combination of one major non-blocked LoS path and multiple NLoS paths [26], given by

$$\begin{aligned} h(t,\tau) = {} & \alpha_0 \exp[j(2\pi f_{D,0} t + \theta_0)]\, \delta(\tau) \\ & + \sum_{l=1}^{L_c - 1} \alpha_l \exp[j(2\pi f_{D,l} t + \theta_l)]\, \delta(\tau - \tau_l), \end{aligned} \quad (14)$$

where α_0 and α_l are the complex value path gains of LoS link and l-th NLoS link, $f_{D,l}$, $l \in \{0, \cdots, L_c\}$ denotes the Doppler shift, θ_0 represents an initial phase, while θ_l is uniformly distributed within $[-\pi, \pi]$, τ_l is the delay of the l-th path. Actually, the Doppler shifts caused by the motion of the satellite can be assumed to be identical for different propagation paths due to the relatively high altitude of the satellite [27], that is, $f_{D,l} = f_D$. It should also be noted that there are long propagation delays in satellite communication systems compared to terrestrial wireless channels, which leads to a much smaller delay spread of the satellite channels than that of the terrestrial wireless channels as observed in measurement results. By taking advantage of the Doppler and delay properties of the satellite propagation channels and performing appropriate time and frequency synchronization at the satellite and the ground user [27], the Doppler shift and time delay can be well compensated [28]–[30].

It should be noted that the LoS component's amplitude can be assumed to be a gamma variable following Nakagami distribution due to the complete or partial blockage of the LoS by buildings, trees, hills, mountains, etc. Therefore, taking the almost perfect Doppler and time delay compensation into consideration, the channel can be simplified to a combination of an NLoS Rayleigh distributed component and an LoS Nakagami distributed component, which is also named Shadowed-Rician (SR) model presented in [31]. The SR channel model has already been proved as an accurate, practical, and applicable tool to evaluate the performance of the satellite propagation environments in various frequency bands, e.g., the UHF-band, L-band, S-band, Ku-band, and Ka-band. Without loss of generality, the probability density function (PDF) of the power gain, $|h(t)|^2$ following SR fading is given as [31],

$$f_{|h(t)|^2}(x) = \alpha(t) \exp(-\beta(t)\, x)\, {}_1F_1(m(t); 1; \delta(t)\, x), x \geq 0, \quad (15)$$

where $\alpha(t) = \left(\frac{2\ b(t) m(t)}{2\ b(t) m(t) + \Omega_h(t)}\right)^{m(t)} / (2\ b(t))$, $\beta(t) = \frac{1}{2\ b(t)}$, and $\delta(t) = \frac{\Omega_h(t)}{2\ b(t)(2\ b(t) m(t) + \Omega_h(t))}$, $\Omega_h(t)$ and $2b(t)$ are the average power of the LoS and multi-path components at time t, respectively, $m(t)$ is the fading severity parameter and ${}_1F_1(\cdot;\cdot;\cdot)$ is the confluent hypergeometric function of first kind [32, Eq. (9.14.1)].

The special cases considering infrequent light shadowing, as well as frequent heavy shadowing, can also be reflected in the SR channel model. For example, by setting $b = 0.158$,

$m = 19.4$, and $\Omega_h = 1.29$, the infrequent shadowing can be represented, while $b = 0.063$, $m = 0.739$, and $\Omega_h = 8.87 \times 10^{-4}$ for heavy shadowing. The channels corresponding to suburban, rural, urban, and open areas can be represented appropriately by setting suitable values for m, where $m = 0$ corresponds to urban areas with complete obstruction of the LoS, while $m = \infty$ corresponds to open areas with no obstruction of the LoS. It should be noted that the atmosphere, such as rainfall, cloud, and various gases, has a strong impact on the space-to-ground transmissions in satellite communication systems, especially for high-frequency bands, like Ka-band. Among them, rain attenuation is [33] the dominant factor, whose power gain commonly follows a log-normal distribution. Specifically, the distribution of the power gain resulted by rain attenuation in dB ξ_{dB} can be written as $\ln(\xi_{\mathrm{dB}}) \sim \mathcal{CN}\left(\mu_\xi, \sigma_\xi^2\right)$, where μ_ξ and σ_ξ are both in dB and represent the log-normal location and scale parameter, respectively. Since this work focuses on investigating the impacts of the satellite's and the Earth's rotations, communication distance, and communication time on the system performance, we will treat the rain attenuation as a constant during the communication process for simplification. The research on the influence of the attenuation factor will be left for our future work.

It is easy to obtain the received SNR at U as

$$\gamma(t) = \frac{P_{\mathrm{S}} \xi^2 |h(t)|^2}{\sigma^2 C d(t)^2}, \tag{16}$$

where $C = \left(\frac{4\pi}{\lambda}\right)^2$ with signal wavelength λ, P_{S} and σ^2 are the transmit power at S and the average power of the additive white Gaussian noise (AWGN) at U, respectively.

IV. System Performance

In this section, we will evaluate the system performance, while considering the position variation on instantaneous OP, instantaneous channel capacity, and throughput.

A. Instantaneous OP

By variable substitution, the PDF and cumulative distribution function (CDF) of the instantaneous SNR can be

$$f_\gamma(x,t) = \alpha(t) \sum_{k=0}^{m(t)-1} \frac{\varsigma(k)}{\bar{\lambda}^{k+1}} d(t)^{2(k+1)} x^k \times \exp\left(-\frac{\beta(t) - \delta(t)}{\bar{\lambda}} d(t)^2 x\right), \tag{17}$$

and

$$F_\gamma(x,t) = 1 - \alpha(t) \sum_{k=0}^{m(t)-1} \varsigma(k) \sum_{p=0}^{k} \frac{k!}{p!} \frac{d(t)^{2p}}{\bar{\lambda}^p} x^p \times (\beta(t) - \delta(t))^{-(k+1-p)} \exp\left(-\frac{\beta(t) - \delta(t)}{\bar{\lambda}} d(t)^2 x\right), \tag{18}$$

respectively, where $\bar{\lambda} = \frac{P_S \xi}{\sigma^2 C}$, $\mathrm{s}(k) = \frac{(-1)^k (1-m(t))_k \delta^k}{(k!)^2}$ and $(n)_k = n(n+1)\cdots(n+k-1)$ is the Pochhammer symbol [32].

Thus, the system OP, $\Pr\{\gamma(t) \le \gamma_{th}\}$, can be presented as

$$F_\gamma(\gamma_{th}, t) = 1 - \alpha(t) \sum_{k=0}^{m(t)-1} \varsigma(k) \sum_{p=0}^{k} \frac{k!}{p!} \frac{d(t)^{2p}}{\bar{\lambda}^p} \gamma_{th}^p \times (\beta(t) - \delta(t))^{-(k+1-p)} \exp\left(-\frac{\beta(t) - \delta(t)}{\bar{\lambda}} d(t)^2 \gamma_{th}\right). \tag{19}$$

For the special case $m(t) = \infty$, the SR channel model will reduced to LoS propagation case. Therefore, OP will only depend on the communication distance that varies with the time, which can be given as

$$\Pr\{\gamma(t) \le \gamma_{th}\} = \Pr\left\{d(t)^2 \ge \frac{P_{\mathrm{S}} |h(t)|^2}{\sigma^2 C \gamma_{th}}\right\}, \tag{20}$$

which will be 0 or 1 at each time t.

B. Instantaneous Channel Capacity

We assume that throughout the time horizon $[t_s, t_e]$, S keeps sending information to U with a constant transmit power P_S. As a result, the instantaneous information bits can be expressed as

$$T(t, |h(t)|^2) = B \log_2\left(1 + \frac{\bar{\lambda} |h(t)|^2}{d(t)^2}\right). \tag{21}$$

By re-presenting ${}_1F_1(\cdot;\cdot;\cdot)$ and taking expectation of the channel, the average instantaneous information bit is

$$\begin{aligned} T(t) &= \mathbb{E}_{h(t)}\{R(t, h(t))\} \\ &= \int_0^\infty R(t, h(t)) f_{|h(t)|^2}(x) dx \\ &= B \int_0^\infty \log_2\left(1 + \frac{\bar{\lambda} x}{d(t)^2}\right) \alpha(t) \\ &\quad \times \exp(-\beta(t) x) {}_1F_1(m; 1; \delta(t) x) dx \\ &= \frac{B\alpha(t)}{\ln 2} \sum_{k=0}^{m(t)-1} \mathrm{s}(k) \int_0^\infty \ln\left(1 + \frac{\bar{\lambda} x}{d(t)^2}\right) \\ &\quad \times x^k \exp\left(-(\beta(t) - \delta(t)) x\right) dx. \end{aligned} \tag{22}$$

To facilitate the derivations, we use the Meijer-G function [34] to represent the logarithmic function and exponential function by $\ln(1+x) = G_{22}^{12}\left(x \middle| \begin{matrix} 1, 1 \\ 1, 0 \end{matrix}\right)$ and $\exp(-x) = G_{01}^{10}\left(x \middle| \begin{matrix} - \\ 0 \end{matrix}\right)$. Using [34], (22) can be calculated as (23) shown at the bottom of the next page.

Similar to the OP, considering the special case $m = \infty$, the instantaneous channel capacity can be rewritten as

$$T(t) = B \log_2\left(1 + \frac{\bar{\lambda}}{d(t)^2}\right), \tag{24}$$

which will varies with the communication distance as the time passes.

C. Throughput

Considering the total communication time, the total amount of the information bits transferred from S to U can be expressed as

$$\begin{aligned} T &= \int_{t_s}^{t_e} T(t)dt \\ &= \int_{t_s}^{t_e} \frac{B\alpha\left(t\right)}{\ln 2} \sum_{k=0}^{m(t)=m-1} \mathrm{s}(k) \left(\frac{\bar{\lambda}}{d\left(t\right)^2}\right)^{-(k+1)} \\ &\quad \times G_{23}^{31}\left(\frac{\left(\beta\left(t\right)-\delta\left(t\right)\right)d\left(t\right)^2}{\bar{\lambda}}\middle| \begin{matrix} -\left(k+1\right),\ -k \\ 0, -(k+1), -(k+1) \end{matrix}\right) dt. \end{aligned} \tag{25}$$

The integration is not solvable considering time-varying SR channels. Thus, we only derive the results for the special case assuming the SR channel is stationary within the communication, that is, $m\left(t\right) = m$ $\Omega_h\left(t\right) = \Omega_h$ and $2b\left(t\right) = 2b$. Combining the expression of $d\left(t\right)^2$ into (25) and using the Chebyshev-Gauss quadrature in the first case, which is presented as $\int_{-1}^{1} \frac{f(x)}{\sqrt{1-x^2}}dx \approx \sum_{i=1}^{W} w_i f\left(x_i\right)$ with $x_i = \cos\left(\frac{2i-1}{2W}\pi\right)$ and the weight $w_i = \frac{\pi}{W}$, the system throughput within the coverage area of S can be rewritten as (26) shown at the bottom of the next page, where $w_i = \frac{\pi}{W_I}$, $\varepsilon_i = \cos\left[(2i-1)\pi/W_I\right]$, $c_1 = \frac{t_e - t_s}{2}$ and $c_2 = \frac{t_e + t_s}{2}$.

When only considering LoS propagation (namely, $m = \infty$), the throughput can be re-calculated as

$$\begin{aligned} T &= \int_{t_s}^{t_e} B\log_2\left(1+\frac{\bar{\lambda}}{d\left(t\right)^2}\right)dt \\ &= Bc_1 \sum_{i=1}^{W_L} w_l\sqrt{1-\epsilon_i^2}\log_2\left(1+\frac{\bar{\lambda}}{d\left(c_1\epsilon_i+c_2\right)^2}\right), \end{aligned} \tag{27}$$

where $w_l = \frac{\pi}{W_L}$, and $\epsilon_i = \cos\left[(2i-1)\pi/W_L\right]$.

D. Simplified Case for Fixed U

Since a low Earth orbit typically takes 90 minutes to revolve around the Earth, which is much faster than the Earth's rotation, we could ignore the position variation during the communication time. In this case, we only need ECI coordinates to demonstrate the positions of S and U, that is, $\omega_e = 0$. Thus, the coordinate of the satellite with ECI coordinate is

$$\begin{aligned} \mathbf{s}_{t,ECI} &= \mathbf{R}_z(-\Omega)\mathbf{R}_x(-i)\mathbf{s}_{t,S} \\ &= \mathbf{R}_z(-\Omega)\mathbf{R}_x(-i)\mathbf{R}_z(\omega_s t)\mathbf{s}_{0,S}, \end{aligned} \tag{28}$$

where each element of the vector $\mathbf{s}_{t,ECI} = \left[\, s_1' \;\; s_2' \;\; s_3 \,\right]^T$ can be calculated as

$$\begin{aligned} s_1' &= H_S\cos\left(-\Omega\right)\cos\left(\omega_s t+v\right) \\ &\quad - H_S\cos\left(i\right)\sin\left(-\Omega\right)\sin\left(\omega_s t+v\right), \end{aligned} \tag{29}$$

and

$$\begin{aligned} s_2' &= H_S\sin\left(-\Omega\right)\cos\left(\omega_s t+v\right) \\ &\quad + H_S\cos\left(-\Omega\right)\cos\left(i\right)\sin\left(\omega_s t+v\right). \end{aligned} \tag{30}$$

Thus, the distance at t is given as

$$\begin{aligned} d'\left(t\right)^2 &= H - 2\left(u_1 s_1' + u_2 s_2' + u_3 s_3\right) \\ &= H + \Upsilon\sin\left(\omega_s t+\beta_s\right), \end{aligned} \tag{31}$$

where $b_1 = -2u_1H_S\cos\left(-\Omega\right) - 2u_2 \;\; H_S\sin\left(-\Omega\right)$, $b_2 = 2u_1H_S\cos\left(i\right)\sin\left(-\Omega\right) - 2u_2H_S\cos\left(-\Omega\right)\cos\left(i\right) - 2u_3H_S\sin\left(-i\right)$, $\Upsilon = -\sqrt{b_1^2+b_2^2}$ and $\beta_s = \arctan\left(\frac{b_1}{b_2}\right) + v$.

1) General Case: Therefore, the instantaneous OP, instantaneous channel capacity and throughput ignoring the mobility of U could be expressed by replacing $d\left(t\right)^2$ by $d'\left(t\right)^2$ in (18), (23) (26), respectively.

2) Special Case for $\gamma(t) < 1$: Moreover, we derive the system throughput for a special case when $\gamma\left(t\right) < 1$. By re-expressing $\ln\left(1+x\right) = \sum_{n=0}^{\infty}\left(-1\right)^{n+1}\frac{x^n}{n}$, the throughput can be re-calculated shown at the bottom of the next page. By adopting [32, Eq. 2.552.3], Θ can be calculated as follows:

$$\begin{aligned} \Theta &= \int_{t_s}^{t_e} \frac{1}{\left[H+\Upsilon\sin\left(\omega_s t+\beta_s\right)\right]^n}dt \\ &= \int_{\omega_s t_s+\beta_s}^{\omega_s t_e+\beta_s} \frac{1}{\omega_s\left[H+\Upsilon\sin\left(y\right)\right]^n}dy \\ &= \frac{1}{\omega_s}F_1\left(\omega_s t_e+\beta_s, \omega_s t_s+\beta_s, n\right), \end{aligned} \tag{33}$$

where $F_1\left(x_1, x_2, n\right)$ is shown at the bottom of the next page, where $F_2\left(x_1, x_2, n, A_n, B_n\right)$ can be expressed as

$$\begin{aligned} &F_2\left(x_1, x_2, n, A_n, B_n\right) \\ &= \frac{1}{\left(n-1\right)\left(H^2-\Upsilon^2\right)} \\ &\quad \times\left[\frac{\left(A_n\Upsilon - HA_n\right)\cos x_1}{\left(H+\Upsilon\sin x_1\right)^{n-1}} - \frac{\left(A_n\Upsilon - HB_n\right)\cos x_2}{\left(H+\Upsilon\sin x_2\right)^{n-1}}\right. \\ &\quad \left.+F_2\left(x_1, x_2, n-1, A_{n-1}, B_{n-1}\right)\right], \end{aligned} \tag{35}$$

where $A_{n-1} = \left(A_nH - B_n\Upsilon\right)(n-1)$, $B_{n-1} = \left(HB_n - \Upsilon A_n\right)(n-2)$ and $F_2\left(x_1, x_2, 1, A_1, B_1\right)$ is shown at the bottom of the next page, where $\mathrm{O} = \frac{A_1\Upsilon - HB_1}{\Upsilon}$.

$$T(t) = \frac{B\alpha\left(t\right)}{\ln 2}\sum_{k=0}^{m(t)-1}\mathrm{s}(k)\int_0^{\infty} x^k G_{22}^{12}\left(\frac{\bar{\lambda}x}{d\left(t\right)^2}\middle|\begin{matrix}1,\,1\\1,\,0\end{matrix}\right) G_{01}^{10}\left(\left(\beta\left(t\right)-\delta\left(t\right)\right)x\middle|\begin{matrix}-\\0\end{matrix}\right)dx$$

$$= \frac{B\alpha\left(t\right)}{\ln 2}\sum_{k=0}^{m(t)-1}\mathrm{s}(k)\left(\frac{\bar{\lambda}}{d\left(t\right)^2}\right)^{-(k+1)} G_{23}^{31}\left(\frac{\left(\beta\left(t\right)-\delta\left(t\right)\right)d\left(t\right)^2}{\bar{\lambda}}\middle|\begin{matrix}-\left(k+1\right),\,-k\\0,\,-\left(k+1\right),\,-\left(k+1\right)\end{matrix}\right) \tag{23}$$

The throughput under LoS propagation case ($m = \infty$) can also be recalculated as

$$T = \frac{B}{\ln 2}\int_{t_s}^{t_e}(-1)^{n+1}\frac{\left(\frac{\bar{\lambda}}{d(t)^2}\right)^{n+1}}{n}dt = \frac{B}{\ln 2}\sum_{n=0}^{\infty}(-1)^{n+1}\frac{\bar{\lambda}^n}{n}\Theta. \quad (37)$$

V. Asymptotic Results

Since the proposed exact expressions for OP, capacity, and throughput in practical system designs and optimizations are a little bit complicated, we will derive some asymptotic closed-form expressions for the instantaneous OP, the instantaneous capacity, and the throughput in simpler forms to gain more insights. The asymptotic closed-form expressions are shown to involve much simpler functions and thus can readily provide direct solutions to some resource optimization problems.

A. Asymptotic Instantaneous OP

As shown in [35], $F_1(m;1;\frac{\delta(t)x}{\bar{\lambda}}) \to 1$ for very large values of $\bar{\lambda}$. Thus, the asymptotic PDF and CDF of $\bar{\gamma} = \bar{\lambda}|h(t)|^2$ becomes

$$f_{\bar{\gamma}}^{A}(x,t) = \frac{\alpha(t)}{\bar{\lambda}}\exp(-\frac{\beta(t)x}{\bar{\lambda}}) \quad (38)$$

and

$$F_{\bar{\gamma}}^{A}(x,t) = \frac{\alpha(t)}{\beta(t)}\left[1-\exp(-\frac{\beta(t)x}{\bar{\lambda}})\right], \quad (39)$$

respectively.

Thus, the asymptotic instantaneous OP can be expressed as

$$F_{\gamma}^{A}(\gamma_{th},t) = \frac{\alpha(t)}{\beta(t)}\left[1-\exp(-\frac{\beta(t)\,d(t)^2\gamma_{th}}{\bar{\lambda}})\right]. \quad (40)$$

B. Asymptotic Instantaneous Channel Capacity

For instantaneous channel capacity, $\ln(1+x)$ could be approximated by $\ln(x)$ when x goes to infinity. Using [32, Eq. 4.352.2], the asymptotic instantaneous channel capacity is

$$\begin{aligned}T^{A}(t) &= \frac{B\alpha(t)}{\ln 2}\sum_{k=0}^{m(t)-1}\mathrm{s}(k)\int_0^{\infty}\ln\left(\frac{\bar{\lambda}x}{d(t)^2}\right)\\ &\quad\times x^k\exp\left(-\left(\beta(t)-\delta(t)\right)x\right)dx\\ &= \frac{B\alpha(t)}{\ln 2}\sum_{k=0}^{m(t)-1}\mathrm{s}(k)\frac{d(t)^{2(k+1)}}{\bar{\lambda}^{k+1}}\int_0^{\infty}\ln(y)\,y^k\\ &\quad\times\exp\left(-\frac{d(t)^2\left(\beta(t)-\delta(t)\right)}{\bar{\lambda}}y\right)dy\\ &= \frac{B\alpha(t)}{\ln 2}\sum_{k=0}^{m(t)-1}\frac{\mathrm{s}(k)k!}{\left(\beta(t)-\delta(t)\right)^{k+1}}\\ &\quad\times\left[C_k-\ln\left(\frac{d(t)^2\left(\beta(t)-\delta(t)\right)}{\bar{\lambda}}\right)\right], \end{aligned} \quad (41)$$

where $C_k = 1+\frac{1}{2}+\frac{1}{3}+\cdots+\frac{1}{k}-C_M$, $C_M = 0.57721566490153286060651 2\ldots$ is Euler's constant.

$$\begin{aligned}T &= \int_{t_s}^{t_e}\frac{B\alpha}{\ln 2}\sum_{k=0}^{m-1}\mathrm{s}(k)\left(\frac{\bar{\lambda}}{d(t)^2}\right)^{-(k+1)}G_{23}^{31}\left(\frac{(\beta-\delta)\,d(t)^2}{\bar{\lambda}}\middle|\begin{matrix}-(k+1),\,-k\\0,\,-(k+1),\,-(k+1)\end{matrix}\right)dt\\ &= c_1\int_{-1}^{1}\frac{B\alpha}{\ln 2}\sum_{k=0}^{m-1}\mathrm{s}(k)\left(\frac{\bar{\lambda}}{d(c_1x+c_2)^2}\right)^{-(k+1)}G_{23}^{31}\left(\frac{(\beta-\delta)\,d(c_1x+c_2)^2}{\bar{\lambda}}\middle|\begin{matrix}-(k+1),\,-k\\0,\,-(k+1),\,-(k+1)\end{matrix}\right)dx\\ &= c_1\sum_{i=1}^{W_I}w_i\sqrt{1-\varepsilon_i^2}\frac{B\alpha}{\ln 2}\sum_{k=0}^{m-1}\mathrm{s}(k)\left(\frac{\bar{\lambda}}{d(c_1\varepsilon_i+c_2)^2}\right)^{-(k+1)}G_{23}^{31}\left(\frac{(\beta-\delta)\,d(c_1\varepsilon_i+c_2)^2}{\bar{\lambda}}\middle|\begin{matrix}-(k+1),\,-k\\0,\,-(k+1),\,-(k+1)\end{matrix}\right)\end{aligned} \quad (26)$$

$$\begin{aligned}T &= \int_{t_s}^{t_e}\frac{B\alpha}{\ln 2}\sum_{k=0}^{m-1}\mathrm{s}(k)\int_0^{\infty}\ln\left(1+\frac{\bar{\lambda}x}{d(t)^2}\right)x^k\exp\left(-(\beta-\delta)x\right)dxdt\\ &= \int_{t_s}^{t_e}\frac{B\alpha}{\ln 2}\sum_{k=0}^{m-1}\mathrm{s}(k)\int_0^{\infty}\sum_{n=0}^{\infty}(-1)^{n+1}\frac{\left(\frac{\bar{\lambda}}{d(t)^2}\right)^{n}}{n}x^{n+k}\exp\left(-(\beta-\delta)x\right)dxdt\\ &= \frac{B\alpha}{\ln 2}\sum_{k=0}^{m-1}\mathrm{s}(k)\sum_{n=0}^{\infty}(-1)^{n+1}\frac{\bar{\lambda}^n}{n}(n+k)!\,(\beta-\delta)^{-(n+k+1)}\underbrace{\int_{t_s}^{t_e}\frac{1}{\left[H+\Upsilon\sin(\omega_s t+\beta)\right]^n}dt}_{\Theta}\end{aligned} \quad (32)$$

$$F_1(x_1,x_2,n) = \frac{1}{(n-1)(H^2-\Upsilon^2)}\left[\frac{\Upsilon\cos x_1}{(H+\Upsilon\sin x_1)^{n-1}}-\frac{\Upsilon\cos x_2}{(H+\Upsilon\sin x_2)^{n-1}}+F_2(x_1,x_2,n-1,(n-1)H,-(n-2)\Upsilon)\right] \quad (34)$$

$$\begin{aligned}&F_2(x_2,x_2,1,A_1,B_1)\\ &= \frac{B_1}{\Upsilon}(x_1-x_2)+\mathrm{O}\begin{cases}\frac{2}{\sqrt{H^2-\Upsilon^2}}\left(\arctan\frac{H\tan\frac{x_1}{2}+\Upsilon}{\sqrt{H^2-\Upsilon^2}}-\arctan\frac{H\tan\frac{x_2}{2}+\Upsilon}{\sqrt{H^2-\Upsilon^2}}\right), & H^2>\Upsilon^2\\ \frac{1}{\sqrt{\Upsilon^2-H^2}}\left(\ln\frac{H\tan\frac{x_1}{2}+\Upsilon-\sqrt{\Upsilon^2-H^2}}{H\tan\frac{x_1}{2}+\Upsilon+\sqrt{\Upsilon^2-H^2}}-\ln\frac{H\tan\frac{x_2}{2}+\Upsilon-\sqrt{\Upsilon^2-H^2}}{H\tan\frac{x_2}{2}+\Upsilon+\sqrt{\Upsilon^2-H^2}}\right), & H^2<\Upsilon^2\end{cases}\end{aligned} \quad (36)$$

From the expression of the asymptotic instantaneous OP and channel capacity, we can see that it is much simpler than the exact instantaneous OP and channel capacity, which just involves the exponential function and logarithm function separately. It will be much easier to apply to optimization problems, like transmit power minimization, which will be discussed in Section VI.

C. Asymptotic Throughput

Accordingly, the asymptotic throughput could be calculated as

$$T^A = \frac{B\alpha}{\ln 2}\sum_{k=0}^{m-1}\frac{\mathrm{s}(k)k!}{(\beta-\delta)^{k+1}}\int_{t_s}^{t_e}\left[C_k - \ln\left(\Psi d\left(t\right)^2\right)\right]\mathrm{d}t = \frac{B\alpha}{\ln 2}\sum_{k=0}^{m-1}\frac{\mathrm{s}(k)k!}{(\beta-\delta)^{k+1}}\left[C_k\Delta t - \int_{t_s}^{t_e}\ln\left(\Psi d\left(t\right)^2\right)\mathrm{d}t\right], \tag{42}$$

where $\Psi = \frac{(\beta-\delta)}{\lambda}$, $\Delta t = t_e - t_s$.

1) Simplified Case: Since the expression of $d\left(t\right)^2$ in the general case is too complicate to calculate, we first derive an asymptotic throughput for the simplified case as

$$\begin{aligned} T^A &= \frac{B\alpha}{\ln 2}\sum_{k=0}^{m-1}\frac{\mathrm{s}(k)k!}{(\beta-\delta)^{k+1}}\left[C_k\Delta t - \int_{t_s}^{t_e}\ln\left(\Psi H + \Psi\Upsilon\sin\left(\omega_s t+\beta_s\right)\right)\mathrm{d}t\right] \\ &= \frac{B\alpha}{\ln 2}\sum_{k=0}^{m-1}\frac{\mathrm{s}(k)k!}{(\beta-\delta)^{k+1}}\left[C_k\Delta t - \ln\left(\Psi H\right)\Delta t - \frac{1}{\omega_s}\int_{\omega_s t_s+\beta_s}^{\omega_s t_e+\beta_s}\ln\left(1+\frac{\Upsilon}{H}\sin\left(y\right)\right)\mathrm{d}y\right]. \end{aligned} \tag{43}$$

Since $d'\left(t\right)^2 = H + \Upsilon\sin\left(\omega_s t+\beta_s\right) > 0$, we can obtain $H+\Upsilon > 0$. As $-\sqrt{b_1^2+b_2^2} < 0$, we have $\left|\frac{\Upsilon}{H}\right| < 1$. In this condition, we could take advantage $\ln\left(1+x\right) = \sum_{n=0}^{\infty}\left(-1\right)^{n+1}\frac{x^n}{n}$ to simplify the calculation. Thus, the asymptotic throughput could be further calculated as

$$\begin{aligned} &T^A \\ &= \frac{B\alpha}{\ln 2}\sum_{k=0}^{m-1}\frac{\mathrm{s}(k)k!}{(\beta-\delta)^{k+1}}\left[C_k\Delta t - \ln\left(\Psi H\right)\Delta t \right. \\ &\quad \left. \underbrace{- \frac{1}{\omega_s}\sum_{n=1}^{\infty}(-1)^{n+1}\frac{\Upsilon^n}{H^n n}\int_{\omega_s t_s+\beta_s}^{\omega_s t_e+\beta_s}\sin\left(y\right)^n\mathrm{d}y}_{I_1}\right] \\ &= \frac{B\alpha}{\ln 2}\sum_{k=0}^{m-1}\frac{\mathrm{s}(k)k!}{(\beta-\delta)^{k+1}}\left[\left(C_k - \ln\Psi H\right)\Delta t - \sum_{n=1}^{\infty}\frac{(-1)^{n+1}}{\omega_s}\right. \\ &\quad \left.\times\frac{\Upsilon^n}{H^n n}\left(F_3\left(\omega_s t_e+\beta_s, n\right) - F_3\left(\omega_s t_s+\beta_s, n\right)\right)\right], \end{aligned} \tag{44}$$

where $F_3\left(x\right)$ is shown at the bottom of the next page.

2) General Case: Similarly, for the general case, we could derive the asymptotic throughput (45), as shown at the bottom of the next page.

To simplify the computation, we only take the first two order of the expansion of the logarithm function as $\lim_{x\to 0}\ln\left(1+x\right) = x - \frac{x^2}{2}$, which could be treated as a lower bound for the throughput. Thus, I could be further calculated (46) and (47), as shown at the bottom of the next page, where I_0 can be easily obtained as

$$\begin{aligned} I_0 = &-\frac{\mu_1}{H\omega_a}\left[\sin\left(\omega_a t_e+\eta_1\right) - \sin\left[\omega_a t_s+\eta_1\right)\right] \\ &-\frac{\mu_2}{H\omega_m}\left[\sin\left(\omega_m t_e+\eta_2\right] - \sin\left[\omega_m t_s+\eta_2\right)\right] \\ &-\frac{\mu_3}{H\omega_s}\left[\cos\left(\omega_s t_e+v\right) - \sin\left(\omega_s t_s+v\right)\right]. \end{aligned} \tag{48}$$

By taking advantage of [32, Eqs. 2.513.5, Eq. 2.513.11], I_1-I_3 can be calculated as

$$\begin{aligned} I_1 &= \int_{\omega_a t_s+\eta_1}^{\omega_a t_e+\eta_1}\frac{\mu_1^2}{2H^2\omega_a}cos^2\left(y\right)\mathrm{d}y \\ &= \frac{\mu_1^2}{8H^2\omega_a}\left[\sin(2\nu_{\max}^1) - \sin(2\nu_{\min}^1) + 2\nu_{\max}^1 - 2\nu_{\min}^1\right], \end{aligned} \tag{49}$$

$$\begin{aligned} I_2 &= \int_{\omega_m t_s+\eta_2}^{\omega_m t_e+\eta_2}\frac{\mu_2^2}{2H^2}\cos^2\left(y\right)\mathrm{d}y \\ &= \frac{\mu_2^2}{8H^2\omega_m}\left[\sin(2\nu_{\max}^2) - \sin(2\nu_{\min}^2) + 2\nu_{\max}^2 - 2\nu_{\min}^2\right] \end{aligned} \tag{50}$$

and

$$\begin{aligned} I_3 &= \int_{\omega_s t_s+v}^{\omega_s t_e+v}\frac{\mu_3^2}{2H^2}\sin^2\left(y\right)\mathrm{d}y \\ &= \frac{\mu_3^2}{8H^2\omega_s}\left[\sin(2\nu_{\min}^3) - \sin(2\nu_{\max}^3) + 2\nu_{\max}^3 - 2\nu_{\min}^3\right], \end{aligned} \tag{51}$$

where $\nu_{\min}^1 = \omega_a t_s+\eta_1$, $\nu_{\max}^2 = \omega_m t_e+\eta_2$, $\nu_{\min}^2 = \omega_m t_s+\eta_2$, $\nu_{\max}^3 = \omega_s t_e + v$ and $\nu_{\min}^3 = \omega_s t_s + v$.

Also, I_4 could be calculated as

$$\begin{aligned} I_4 &= \int_{t_s}^{t_e}\frac{\mu_1\mu_2}{H^2}cos\left(\omega_a t+\eta_1\right)\cos\left(\omega_m t+\eta_2\right)\mathrm{d}t \\ &= \frac{\mu_1\mu_2}{H^2}\left[F_4(\omega_a,\eta_1,\omega_m,\eta_2,t_e) - F_4(\omega_a,\eta_1,\omega_m,\eta_2,t_s)\right], \end{aligned} \tag{52}$$

where $F_4\left(a,b,c,d,x\right)$ is given by [32, 2.532.3] as

$$F_4\left(a,b,c,d,x\right) = \frac{\sin[(a-c)x+b-d]}{2(a-c)} - \frac{\sin[(a+c)x+b+d]}{2(a+c)}. \tag{53}$$

Furthermore, in the same way I_5-I_6 could be calculated as

$$I_5 = \frac{\mu_1\mu_3}{H^2}\left[F_5(\omega_s,v,\omega_a,\eta_1,t_e) - F_5(\omega_s,v,\omega_a,\eta_1,t_s)\right] \tag{54}$$

and

$$I_6 = \frac{\mu_2\mu_3}{H^2}\left[F_5(\omega_s, v, \omega_m, \eta_2, t_e) - F_5(\omega_s, v, \omega_m, \eta_2, t_s)\right], \tag{55}$$

where $F_5\left(a, b, c, d, x\right)$ is given by [32, 2.532.2] as

$$F_5\left(a, b, c, d, x\right) = -\frac{\cos[(a-c)x + b - d]}{2(a-c)} - \frac{\cos[(a+c)x + b + d]}{2(a+c)}. \tag{56}$$

Substituting (48) (49), (50), (51), (52), (54) and (55) into (47), we could obtain the asymptotic throughput for the general case.

From the asymptotic results shown in (44) and (46), we can see that the minimum transmit power that satisfies a certain throughput threshold can be derived easily. The closed-form solution will be given in Section VI.

VI. Applications and Future Directions

In this subsection, we give some applications for our derived results in satellite communication, which is also the future directions.

A. Resource Allocation Problems

The resource allocation problems are mainly solved based on two kinds of assumptions about channel state information (CSI), that is, statistical CSI [36], and perfect CSI [37]. Due to the communication distance variation in our considered satellite communication system, we focus on the discussion about the resource allocation under the assumption that perfect CSI is available for better demonstration purpose. The system model and derived results can provide an easier way to allocate resources. For example, the transmit power can be adjusted to satisfy the quality of service (QoS) assuming available CSI by solving the following optimization problems:

$$\begin{aligned}(\mathbf{P1}):\ &\text{Given}:\ \text{CSI}, \gamma_{\rm th}, \mathbf{s}_{0,\rm S}, \mathbf{u}\\ &\text{Minimize}:\ P_S\left(t\right)\\ &\text{Subject to}:\ F\left(\gamma_{th}, t\right) \le P_o,\\ &\qquad 0 < P_S\left(t\right) \le P_{\max},\end{aligned} \tag{57}$$

where P_o is the OP threshold and $P_{\max}$ denotes the maximum transmit power.

$$\begin{aligned}(\mathbf{P2}):\ &\text{Given}:\ \text{CSI}, T_{th}, \mathbf{s}_{0,S}, \mathbf{u}\\ &\text{Minimize}:\ P_S\left(t\right)\\ &\text{Subject to}:\ T\left(t\right) \ge T_{th},\\ &\qquad 0 < P_S\left(t\right) \le P_{\max},\end{aligned} \tag{58}$$

where T_{th} denotes the capacity threshold.

It should be noted that the minimal transmit power for the above two optimization problems occurs when $F\left(\gamma_{th}, t\right) = P_o$ and $T\left(t\right) = T_{th}$. Based on the derived instantaneous OP and capacity shown in (18) and (23), the proposed optimization problem can be transformed to the problems of solving equations $F\left(\gamma_{th}, t\right) = P_o$ and $T\left(t\right) = T_{th}$. Although we cannot derive the closed-form for the optimal solution, its numerical results can be easily solved by many software, like MATLAB.

$$F_3\left(x, l\right) = \begin{cases} -\dfrac{\cos x}{2\ l}\left\{\sin^{2\ l-1} x + \displaystyle\sum_{k=1}^{l-1} \frac{(2\ l-1)(2\ l-3)\ldots(2\ l-2\ k+1)}{2^k(l-1)(l-2)\ldots(l-k)} \sin^{2\ l-2\ k-1} x\right\} + \dfrac{(2\ l-1)!!}{2\ l!}x, k \text{ is even} \\ -\dfrac{\cos x}{2\ l+1}\left\{\sin^{2\ l} x + \displaystyle\sum_{k=0}^{l-1} \frac{2^{k+1} l(l-1)\ldots(l-k)}{(2\ l-1)(2\ l-3)\ldots(2\ l-2\ k-1)} \sin^{2\ l-2\ k-2} x\right\}, k \text{ is odd} \end{cases} \tag{45}$$

$$T^A = \frac{B\alpha}{\ln 2}\sum_{k=0}^{m-1} \mathrm{s}(k) k! \left[(C_k - \ln\left(\Psi H\right))\Delta t - \frac{1}{\omega_s}\underbrace{\int_{t_s}^{t_e} \ln\left(1 + \frac{\mu_1}{H} cos\left(\omega_a t + \eta_1\right) + \frac{\mu_2}{H}\cos\left(\omega_m t + \eta_2\right) + \frac{\mu_3}{H}\sin\left(\omega_s t + v\right)\right) \mathrm{d}t}_{I_2}\right] \tag{46}$$

$$\begin{aligned} I_2 = &\underbrace{\int_{t_s}^{t_e}\left[\frac{\mu_1}{H}\cos\left(\omega_a t + \eta_1\right) + \frac{\mu_2}{H}\cos\left(\omega_m t + \eta_2\right) + \frac{\mu_3}{H}\sin\left(\omega_s t + v\right)\right]\mathrm{d}t}_{I_0} - \underbrace{\int_{t_s}^{t_e} \frac{\mu_1^2}{2H^2} cos^2\left(\omega_a t + \eta_1\right)\mathrm{d}t}_{I_1} \\ &- \underbrace{\int_{t_s}^{t_e} \frac{\mu_2^2}{2H^2}\cos^2\left(\omega_m t + \eta_2\right)\mathrm{d}t}_{I_2} - \underbrace{\int_{t_s}^{t_e} \frac{\mu_3^2}{2H^2}\sin^2\left(\omega_s t + v\right)\mathrm{d}t}_{I_3} - \underbrace{\int_{t_s}^{t_e} \frac{\mu_1\mu_2}{H^2} cos\left(\omega_a t + \eta_1\right)\cos\left(\omega_m t + \eta_2\right)\mathrm{d}t}_{I_4} \\ &- \underbrace{\int_{t_s}^{t_e} \frac{\mu_1\mu_3}{H^2} cos\left(\omega_a t + \eta_1\right)\sin\left(\omega_s t + v\right)\mathrm{d}t}_{I_5} - \underbrace{\int_{t_s}^{t_e} \frac{\mu_2\mu_3}{H^2}\cos\left(\omega_m t + \eta_2\right)\sin\left(\omega_s t + v\right)\mathrm{d}t}_{I_6} \end{aligned} \tag{47}$$

By taking advantage of the asymptotic results, the sub-optimal solution in closed-form expression can be obtained. Let the asymptotic OP shown in (40) equals to P_o, one can derive the minimum transmit power satisfying the outage requirement as

$$P_S(t) = \frac{\sigma^2 C\beta(t) d(t)^2 \gamma_{th}}{-\ln\{1-\frac{P_o\beta(t)}{\alpha(t)}\}}. \tag{59}$$

Similarly, let the asymptotic capacity shown in (41) equals to T_{th}, we can derive the minimum transmit power that satisfies the required capacity as

$$P_S = \frac{\sigma^2\ Cd(t)^2(\beta(t)-\delta(t))}{\exp\left\{\frac{1}{m}\sum_{k=0}^{m-1}\frac{\mathrm{s}(k)k!}{m(\beta(t)-\delta(t))^{k+1}}C_k - \frac{\ln 2}{B\alpha(t)}T_{th}\right\}}. \tag{60}$$

Moreover, the minimum transmit power can also be calculated to achieve the required throughput within the communication coverage by solving the following optimization problem:

$$\begin{aligned}(\mathbf{P3}):\ &\text{Given}:\ \mathrm{CSI}, \mathrm{T_{th}}, \mathbf{s}_{0,\mathrm{S}}, \mathbf{u}\\ &\text{Minimize}:\ \mathrm{P_S}\\ &\text{Subject to}:\ \mathrm{T}\geq \mathrm{T_{th}},\\ &\qquad 0<P_S\leq P_{\max},\end{aligned} \tag{61}$$

Similarly, the proposed optimization problems could be solved easily by software based on the satellite coordinate and the derived closed-form expressions shown in (26). It should be noted that the derived transmit power is not instantaneous but for a satellite visibility window.

By observing the asymptotic throughput for the simplified case and general case shown in (44) and (46), the minimal transmit power can also be obtained in closed-form as

$$P_S = \frac{\sigma^2 CH(\beta-\delta)}{\exp\left\{\frac{1}{m\Delta t}\sum_{k=0}^{m-1}\frac{\mathrm{s}(k)k!}{(\beta-\delta)^{k+1}}[C_k\Delta t - I_1] - \frac{\ln 2}{mB\alpha\Delta t}T_{th}\right\}}, \tag{62}$$

and

$$P_S = \frac{\sigma^2 CH(\beta-\delta)}{\exp\left\{\frac{1}{m\Delta t}\sum_{k=0}^{m-1}\mathrm{s}(k)k!\left[C_k\Delta t - \frac{1}{\omega_s}I_2\right] - \frac{\ln 2T_{th}}{mB\alpha\Delta t}\right\}}. \tag{63}$$

It should be noted that the closed-form solutions approach the optimal solution as the overall system performance improves.

B. Multiple Satellite Communication System

Recently, mega-constellations systems have been proposed and being developed as a promising way to construct global connectivity [38]. Such satellite communication systems are designed to be composed of thousands of mass-produced small satellites working in combination with ground transceivers. Therefore, multi-satellite communication systems are an interesting and promising research direction. Although we only analyze the system performance while considering one satellite and one ground user, the analysis can be readily expanded to multi-satellite scenarios. In such a case, the ground device can be served by several satellites simultaneously in different orbits or the same orbits (e.g., LEO satellites). In other words, under that case, the ground device is located in the intersection area of multiple satellites with different altitudes and rotation speeds or the same altitude/rotation speed. The device on the ground can adopt combining schemes to improve its communication quality when several satellites are active and send the same information bits. For example, the ground user is located in a coverage area, where it can be served by $N(t)$ satellites simultaneously. The number of serving satellites $N(t)$ varies over time because of the mobility of the satellite and the Earth rotation. The received SNR at the ground user for the i-th satellite can be expressed as

$$\gamma_i(t) = \frac{P_{\mathrm{S},i}(t)|h_i(t)|^2}{\sigma^2 d_i(t)^2}. \tag{64}$$

To improve the communication quality, the ground user can adopt the maximal ratio combining scheme, generalized selection combining scheme, or selection combining scheme.

On the other hand, satellites sharing the same frequency may serve different devices within their overlapping coverage area, which leads to interference to the ground devices located in the same area that communicate with different satellites. Considering the target ground receiver located in the intersection area interfered by $N_I(t)$ satellites, the received SNR can be re-expressed as

$$\gamma(t) = \frac{\frac{P_{\mathrm{S}}(t)}{d(t)^2}|h(t)|^2}{\sum_{i=1}^{N_I(t)}\frac{P_{\mathrm{S},i}(t)}{d_i(t)^2}|h_i(t)|^2+\sigma^2}. \tag{65}$$

Since each satellite's serving time is different, the instantaneous system performance and throughput within different satellite visibility windows are also varying.

Another interesting problem that can be introduced is satellite handover. Based on the proposed satellite coordinate, the rotation routing of satellites can be predicted as well as the serving time. By acknowledging the users' position, the start point of connection time and the endpoint can be accessed. The next satellite can reserve enough resources to perform a more fluent satellite handover. For example, there are 12 LEO satellites uniformly distributed in the same orbit, with same $\beta_{\max} = \frac{2\pi}{9}$. Under the (P, Q, W) coordinate, the positions of satellites are assumed to be $\left(H_S\cos\left(\frac{\pi}{6}i\right), H_S\cos\left(\frac{\pi}{6}i\right), 0\right)$, $i \in 1, \cdots, 12$. Based on the derived distance expression over time shown in (13) and maximal communication distance $d_{\max} = \frac{H_S - H_E}{\cos\left(\frac{2\pi}{9}\right)}$. The start point and endpoint for the connection between i-th satellite and the ground user can be obtained by solving the equation $d(t) = d_{\max}$. It should be noted that there are some time overlaps between adjacent satellites because of the coverage overlap. Based on the derived time and satellite visibility window, the controller can schedule the active satellite for the ground user and implement satellite handover appropriately. It is just a simple example of satellite handover based on our derived results considering a single orbit. In a more realistic case, there are several orbits with different altitudes and directions that cross the target area

simultaneously. They will act as a transmitter or an interferer. Further discussions and novel handover schemes will be left for our future works.

Moreover, an LEO satellite can only serve the devices within a limited satellite visibility window. The information bits may not be delivered by one satellite. When there are a large amount of data packets for delivery, they may be allocated to several satellites to deliver to the ground user at the same time or subsequently. The described satellite coordinate can predict the rotation routing of satellites and allocate the transmissions in advance.

C. Mobile Devices

In practice, there are mobile users on the ground or flying over the air [39], [40], resulting in varying positions over time. By taking the moving speed and direction into consideration, the system performance can be analyzed in a similar way. Especially for fixed route moving devices, like trains, flights, and buses, the resources can be allocated properly in advance according to the fixed route and moving speed. For example, assuming a user moves on the ground with azimuthal angle and polar angle variations $\Delta\theta_u(t)$ and $\Delta\varphi_u(t)$ with ECEF coordinates

$$u_1 = H_E \sin(\theta_u + \Delta\theta_u(t)) \cos(\varphi_u + \Delta\varphi_u(t)), \quad (66)$$

$$u_2 = H_E \sin(\theta_u + \Delta\theta_u(t)) \sin(\varphi_u + \Delta\varphi_u(t)), \quad (67)$$

and

$$u_3 = H_E \cos(\theta_u + \Delta\theta_u(t)) \quad (68)$$

of the user at t. By replacing θ_u and φ_u in (13) by $\theta_u + \Delta\theta_u(t)$ and $\varphi_u + \Delta\varphi_u(t)$, the instantaneous distance can also be derived. Accordingly, the instantaneous OP and capacity as well as the system throughput can also be derived. The flying devices over the air like flying cars, unmanned aerial vehicles (UAVs), high-altitude platforms (HAPs) also can be analyzed in the same way with different radial distance. Except for the fixed route case, the user may have random movements within a satellite visibility window. One way to model the randomness position is to assume θ_u and φ_u are uniformly distributed within $[\theta_1, \theta_2]$ and $[\varphi_1, \varphi_2]$ respectively, where $0 \le \theta_1 \le \theta_2 \le \pi$ and $0 \le \varphi_1 \le \varphi_2 \le 2\pi$.

Furthermore, due to the high path loss over the propagation in the satellite communication systems, there will be cooperation devices like relays, reconfigurable intelligent surfaces (RISs) to assist the communications. Whether they are fixed or moving, and no matter whether they are in the air or on the ground or underwater, the system performance can always be analyzed through the results replacing different communication distances. The resource allocation and satellite handover scheme can also be further discussed accordingly.

VII. Extreme Short Communication Duration

The position of U, the rotation rate of S, and the position of the orbit may cause a short communication time. In this case, the channel fading is time-varying rather than ergodic and time-fixed. In other words, the channel state cannot be ergodic as suggested by the channel distribution within a short satellite visibility window. The experienced channel within with satellite visibility window $t_e - t_s$ can be expressed as $h(t) \in h\left(t_s + \frac{t_e - t_s}{n}\right)$, $n = 1, \cdots, N$, where N is a small integer number. The worst occasion happens when $N = 1$, that is, $h(t) = h(t_e)$, which means that the channel condition is fixed within a short satellite visibility window $t_e - t_s$. Since the communication happens within a short satellite visibility window, the distance is approximated to the maximum communication distance, which is $d_{\max}$. Thus, the throughput could be expressed as

$$T_s = \frac{BT}{N} \sum_{n=1}^{N} \log_2 \left(1 + \frac{P_S \xi^2 \left|h\left(t_s + \frac{t_e - t_s}{n}\right)\right|^2}{\sigma^2 C d_{\max}^2}\right). \quad (69)$$

In this case, the average OP could be counted as

$$P_{out} = \frac{1}{N} \sum_{n=1}^{N} \Pr\left\{\frac{P_S \xi^2 \left|h\left(t_s + \frac{t_e - t_s}{n}\right)\right|^2}{\sigma^2 C d_{\max}^2} < \gamma_{th}\right\}. \quad (70)$$

It should be noted that, since the channel is not ergodic within T, the throughput and the OP would be different compared to the general case, which can be clearly seen from the numerical results presented in the next section.

VIII. Numerical Results

In this section, Monte-Carlo simulation and analytical results will be provided to study the performance of the considered system and verify the proposed analytical expression. In the following, we denote the case considering the Earth's rotation as ER, while the one ignoring the Earth's rotation is named as WER.

A. Instantaneous OP

Firstly, we study the instantaneous OP under parameter settings: $f = 12$GHz, $P_S = 50$ dBW, $N_0 = -154$ dB, $b = 0.158$, $\Omega_h = 1.29$, $m = 19$, $\Omega = \pi/3$, $i = \pi/6$, $v = \pi/4$, $\theta_u = \pi/2$, $\varphi_u = \pi/8$, $\omega_S = 0.025$ deg/s, $\beta_{\max} = 35^\circ$ and $H_S = 16000$ km. As shown in Fig. 3, the instantaneous OP mainly depends on the communication distance between S and U. There is an apparent difference in communication distance for WER and ER, especially when the satellite orbit is high, and the rotation speed is slow. As time goes by, the OP of WER will be periodic while the OP of ER changes in each rotation period, which is caused by the Earth's rotation. Moreover, the gaps between the instantaneous OP and the distance of ER and WER become large firstly, then decrease. After several periods, the gaps go back to the same as the first one, which implies that the distance difference between ER and WER is a periodic function. It also proved that we should not ignore the distance variation in the realistic scenario since it brings performance variation and outage. In Fig. 4, we could see that the asymptotic OP matches perfectly with the exact OP in high SNR regime with $b = \Omega_h = 15$ dB and $m = 2$. Moreover, the communication time could be greatly reduced by increasing the rotation speed of the satellite, because U stays more shortly in the coverage area. Moreover, we conduct the experiment on the optimal power allocation, which is

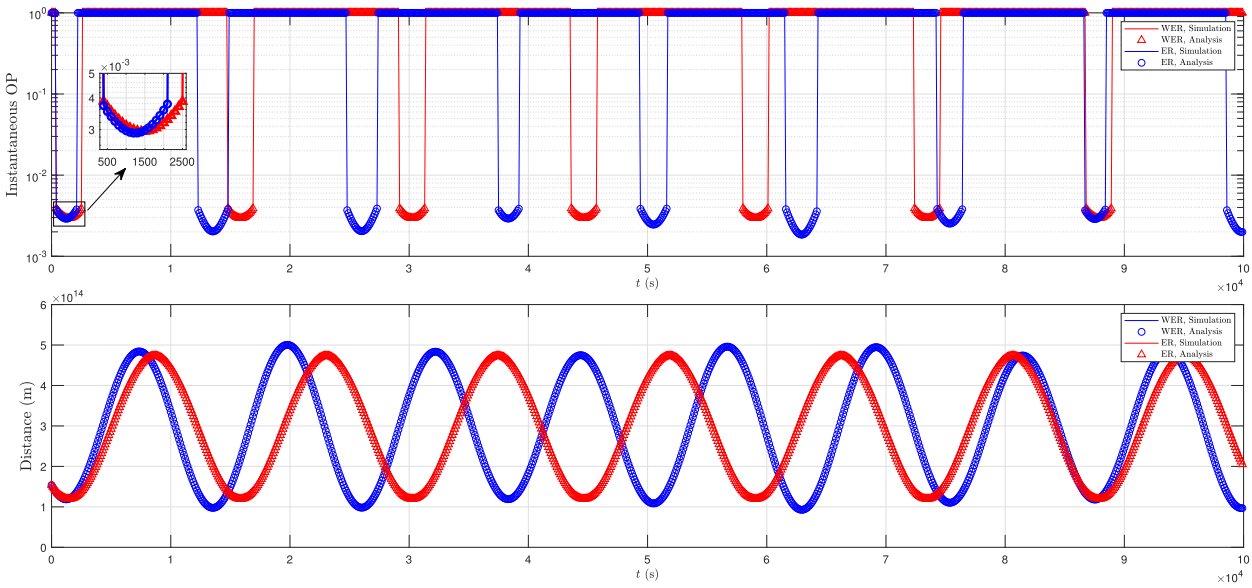

Fig. 3. ER instantaneous OP vs WER instantaneous OP and ER instantaneous distance vs WER instantaneous distance.

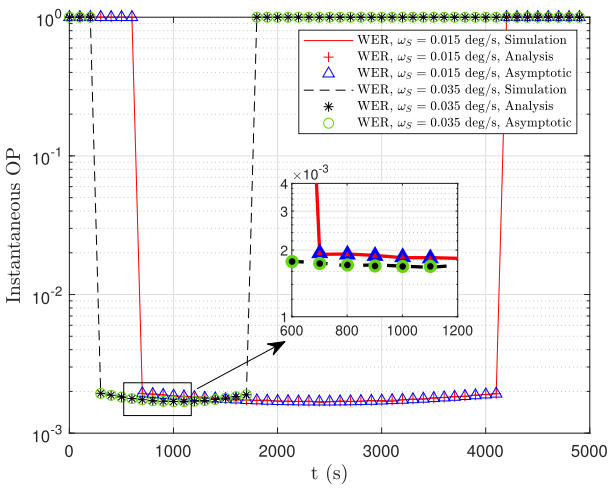

Fig. 4. WER instantaneous OP for various ω_S.

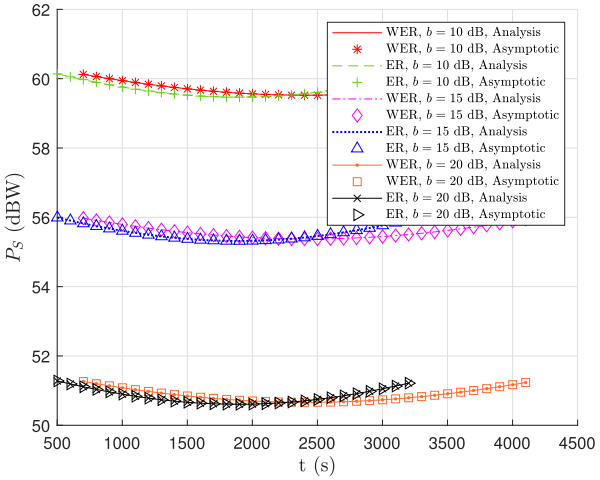

Fig. 5. ER instantaneous transmit power vs WER instantaneous transmit power for various b.

shown in Fig. 5. Based on the derived closed-expression of OP, we use the function "vpasolve" in MATLAB to get the exact minimum transmit power to make the OP satisfy the system requirement, that is, $P_o = 0.001$. We can see that the transmit power decreases firstly and then increases, which varies corresponding to the communication distance. We also adopt the closed-form solution shown in (59) derived by the asymptotic OP, which is shown to be accurate in the high SNR regime.

B. Instantaneous Channel Capacity

By re-setting $b = 0.063$, $\Omega_h = 8.97 \times 10^{-4}$, $m = 1$, $\Omega = \pi/12$, $i = \pi/10$, $v = 0$, $\theta_u = \pi/2$, $\varphi_u = 0$ and $H_S = 7800$ km, the instantaneous channel capacity variation is shown in Fig. 6. We can see that the instantaneous channel capacities in the first satellite visibility window for different satellite rotation rates are very close. Moreover, the fast-rotating satellite could fall into the next satellite visibility window earlier. There are apparent transmission duration and communication distance variations among each satellite visibility window. In Fig. 7 with resetting parameters $b = \Omega_h = 15$ dB and $m = 2$, we could see that the instantaneous channel capacity in the first satellite visibility window under ER is the same as the one under WER case. In the following communication time, there are apparent differences between the performance under ER and the one under WER. We could conclude that even if the satellite has a high rotation speed, the Earth's rotation could only be ignored in the first satellite visibility window. Also, under WER, the instantaneous channel capacity could remain the same in every satellite visibility window, while the one under ER keeps varying.

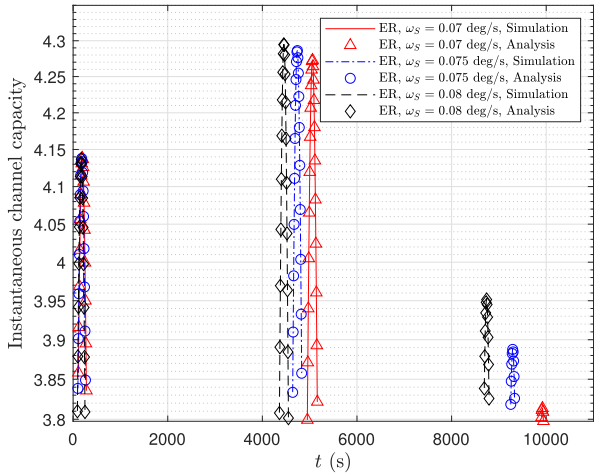

Fig. 6. ER instantaneous channel capacity for various ω_S.

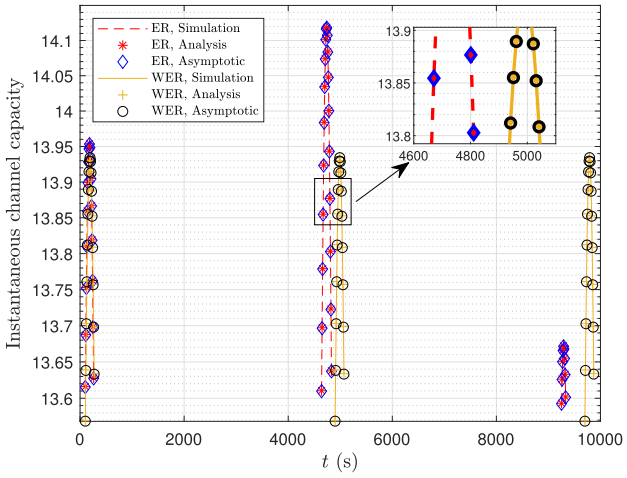

Fig. 7. ER instantaneous channel capacity vs WER instantaneous channel capacity.

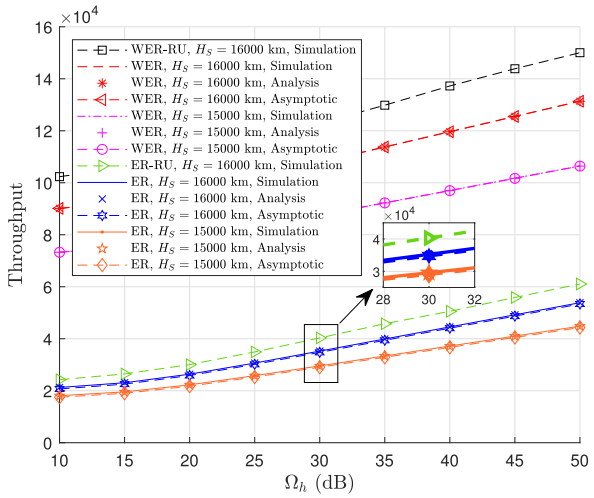

Fig. 8. ER throughput vs WER throughput for various H_S.

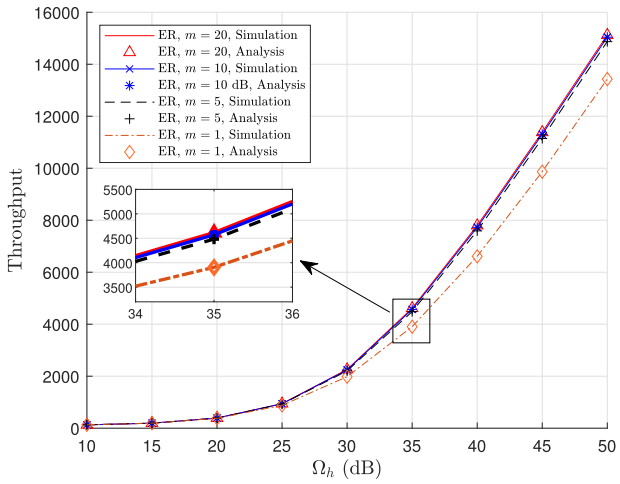

Fig. 9. ER throughput for various m.

C. Throughput

By setting $P_S = 50$ dBW, $b = 15$ dB, communication time $\Delta t = 5000$ seconds and keeping other parameters in subsection A, we verify the correctness of our proposed throughput expression. In Fig. 8, we could see that the throughput increases as the height of the satellite's orbit increases because high orbit leads to the large coverage area and long communication time. Moreover, WER gains higher throughput than ER caused by longer communication time and shorter communication distance, which could be treated as an upper bound for a realistic case. The asymptotic throughput matches the exact one closely. We also compare the throughput with the cases considering the random moving user, named WER-RU and ER-RU. The case is just a simple example, where the mobile user changes its position randomly within a limited area $\theta_u \in \left[\frac{\pi}{2}, \frac{\pi}{2} + \frac{\pi}{20}\right]$, $\varphi_u \in \left[\frac{\pi}{8}, \frac{\pi}{8} + \frac{\pi}{20}\right]$. It can be seen that the cases considering mobile users may lead to higher throughput within a limited time, because its random position may lead to shorter communication distance or longer communication time. It should be noted that the users' mobility can lead to better throughput or much worse throughput, which depends on practical movements. As seen in Fig. 9 with resetting parameters $P_S = 10$ dBW, the system throughput increases as the fading severity parameter increases due to stronger LoS component. However, it does not increase apparently when m is bigger than 5. From Figs. 8-9, it is obvious that better LoS channel conditions could greatly improve system performance.

D. Extreme Short Communication Duration

In this part, we compare the throughput and the OP under a non-ergodic channel with the ones under an ergodic channel with parameter setting: $b = \Omega_h = 5$ dB and the other same parameters in Part A of this section. As shown in Fig. 10, the throughput under non-ergodic cases could be higher or lower than the ergodic case since the instantaneous channel could be better or worse than the ergodic one. Similarly, in Fig. 11, the OP also depends on the instantaneous channel quality, although with the same fixed channel power gain. It should be noted that the OP could only take N results,

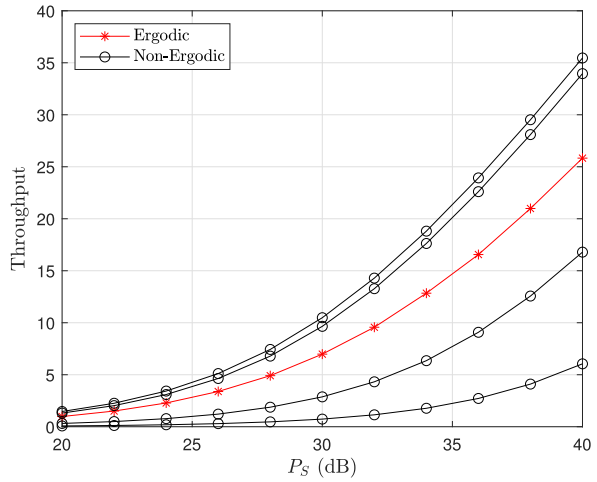

Fig. 10. Ergodic throughput vs non-ergodic throughput.

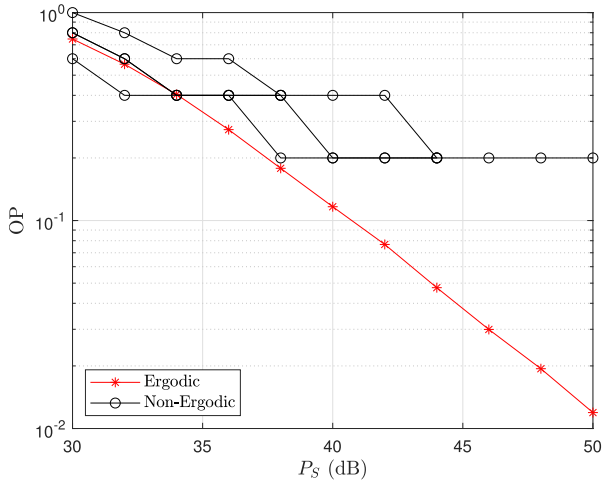

Fig. 11. Ergodic OP vs non-ergodic OP with $N = 5$.

that is, $\frac{n}{N}$, $n = 0, \cdots, N$. We could conclude that the throughput and the OP within a short transmission time could not be represented by the ones of the general case anymore. Moreover, the throughput and the OP in both cases could be greatly improved by increasing the transmit power at the satellite.

IX. Conclusion

Taking the Earth's rotation and satellite rotation into account, a non-stationary satellite communication system is modeled. We study the instantaneous OP, instantaneous channel capacity, and throughput during the finite satellite visibility window of the proposed non-stationary satellite communication system. A simpler case without the Earth's rotation is also studied in this paper, as well as asymptotic results for both cases. Applications involved with our derived results and future research direction are also discussed. Considering a short satellite visibility window, new definitions for throughput and OP are proposed.

Observing from the numerical results, some remarks can be achieved as follows:

1) The distance variation shows a great influence on the system performance, because of the unavoidable path loss.

2) There is an apparent difference in the communication distance for WER and ER, which leads to performance gaps. Also, the distance difference between ER and WER is a periodic function.

3) A faster rotation speed of the satellite leads to shorter communication duration because a shorter satellite visibility window for U is available staying in the coverage area of the satellite. Moreover, the fast-rotating satellite could fall into the next satellite visibility window earlier.

4) Even with a high satellite rotation speed, the Earth's rotation could only be ignored in the first satellite visibility window.

5) A large radius of satellite orbit brings an improved throughput. However, it can be eliminated by high path loss.

6) The throughput of WER could be treated as an upper bound for the throughput of ER.

7) The throughput and the OP within short transmission time under non-ergodic channel fading could not be represented by the ones under ergodic channel fading.

8) The asymptotic results can be used to solve the transmit power allocation problem in closed-form solutions.

References

[1] A. Guidotti *et al.*, "Architectures and key technical challenges for 5G systems incorporating satellites," *IEEE Trans. Veh. Technol.*, vol. 68, no. 3, pp. 2624–2639, Mar. 2019.

[2] M. Giordani and M. Zorzi, "Satellite communication at millimeter waves: A key enabler of the 6G era," in *Proc. Int. Conf. Comput., Netw. Commun. (ICNC)*, Feb. 2020, pp. 383–388.

[3] S. Dang, O. Amin, B. Shihada, and M.-S. Alouini, "What should 6G be?" *Nature Electron.*, vol. 3, no. 1, pp. 20–29, Jan. 2020.

[4] E. Yaacoub and M. Alouini, "A key 6G challenge and opportunity—Connecting the base of the pyramid: A survey on rural connectivity," *Proc. IEEE*, vol. 108, no. 4, pp. 533–582, Mar. 2020.

[5] P. Chini, G. Giambene, and S. Kota, "A survey on mobile satellite systems," *Int. J. Satell. Commun. Netw.*, vol. 28, no. 1, pp. 29–57, Jan. 2010.

[6] K. An, Y. Li, X. Yan, and T. Liang, "On the performance of cache-enabled hybrid satellite-terrestrial relay networks," *IEEE Wireless Commun. Lett.*, vol. 8, no. 5, pp. 1506–1509, Oct. 2019.

[7] P. K. Upadhyay and P. K. Sharma, "Max-max user-relay selection scheme in multiuser and multirelay hybrid satellite-terrestrial relay systems," *IEEE Commun. Lett.*, vol. 20, no. 2, pp. 268–271, Feb. 2016.

[8] K. An, M. Lin, and T. Liang, "On the performance of multiuser hybrid satellite-terrestrial relay networks with opportunistic scheduling," *IEEE Commun. Lett.*, vol. 19, no. 10, pp. 1722–1725, Oct. 2015.

[9] X. Wu, M. Lin, H. Kong, Q. Huang, J.-Y. Wang, and P. K. Upadhyay, "Outage performance for multiuser threshold-based DF satellite relaying," *IEEE Access*, vol. 7, pp. 103142–103152, 2019.

[10] K. Guo, B. Zhang, Y. Huang, and D. Guo, "Performance analysis of two-way satellite terrestrial relay networks with hardware impairments," *IEEE Wireless Commun. Lett.*, vol. 6, no. 4, pp. 430–433, Aug. 2017.

[11] Y. Ruan, Y. Li, C.-X. Wang, R. Zhang, and H. Zhang, "Effective capacity analysis for underlay cognitive satellite-terrestrial networks," in *Proc. IEEE Int. Conf. Commun. (ICC)*, May 2017, pp. 1–6.

[12] X. Yan, H. Xiao, K. An, G. Zheng, and S. Chatzinotas, "Ergodic capacity of NOMA-based uplink satellite networks with randomly deployed users," *IEEE Syst. J.*, vol. 14, no. 3, pp. 3343–3350, Sep. 2020.

[13] G. Alfano, A. De Maio, and A. M. Tulino, "A theoretical framework for LMS MIMO communication systems performance analysis," *IEEE Trans. Inf. Theory*, vol. 56, no. 11, pp. 5614–5630, Nov. 2010.

[14] P. Loreti and M. Luglio, "Interference evaluations and simulations for multisatellite multibeam systems," *Int. J. Satell. Commun.*, vol. 20, no. 4, pp. 261–281, 2002.

[15] F. Vatalaro, G. E. Corazza, C. Caini, and C. Ferrarelli, "Analysis of LEO, MEO, and GEO global mobile satellite systems in the presence of interference and fading," *IEEE J. Sel. Areas Commun.*, vol. 13, no. 2, pp. 291–300, Feb. 1995.
[16] W. Zhaofeng, H. Guyu, Y. Seyedi, and J. Fenglin, "A simple real-time handover management in the mobile satellite communication networks," in *Proc. 17th Asia–Pacific Netw. Oper. Manage. Symp. (APNOMS)*, Aug. 2015, pp. 175–179.
[17] J. Xu, J.-H. Jong, C. Ravishankar, A. Noerpel, and Y. Vasavada, "Algorithm and analysis of using GPS for a hybrid mobile satellite terminal," in *Proc. MILCOM Mil. Commun. Conf.*, Nov. 2011, pp. 792–796.
[18] K. Ito, K. Hoshinoo, and M. Ito, "Differential positioning experiment using two geostationary satellites," *IEEE Trans. Aerosp. Electron. Syst.*, vol. 35, no. 3, pp. 866–878, Jul. 1999.
[19] C. T. Ardito, J. J. Morales, J. Khalife, A. A. Abdallah, and Z. M. Kassas, "Performance evaluation of navigation using LEO satellite signals with periodically transmitted satellite positions," in *Proc. Int. Tech. Meeting Inst. Navigat.*, Feb. 2019, pp. 306–318.
[20] U. K. Acharjee, A. Ahmed, and S. Rafique, "Performance analysis of navigation by the integration of GPS-24 with LEO & GEO," in *Proc. 10th Int. Conf. Comput. Inf. Technol.*, Dec. 2007, pp. 1–6.
[21] L. Ma, C. Hu, and J. Pei, "Polarization tracking study of Earth station in satellite communications," *Sci. Res.*, vol. 5, no. 1, pp. 10–19, 2016.
[22] F. Rahman and J. A. Farrell, "Earth-centered Earth-fixed (ECEF) vehicle state estimation performance," in *Proc. IEEE Conf. Control Technol. Appl. (CCTA)*, Aug. 2019, pp. 27–32.
[23] M. Seppänen, J. Ala-Luhtala, R. Piché, S. Martikainen, and S. Ali-Löytty, "Autonomous prediction of GPS and GLONASS satellite orbits," *Navigation*, vol. 59, no. 2, pp. 119–134, Jun. 2012.
[24] M. S. Grewal, L. R. Weill, and A. P. Andrews, *Global Positioning Systems, Inertial Navigation, and Integration*. Hoboken, NJ, USA: Wiley, 2007.
[25] *Study on New Radio (NR) to Support Non-Terrestrial Networks*, Standard TR 38.811 (Release 15), 3GPP, 2020.
[26] J. Lin, Z. Hou, Y. Zhou, L. Tian, and J. Shi, "Map estimation based on Doppler characterization in broadband and mobile LEO satellite communications," in *Proc. IEEE 83rd Veh. Technol. Conf. (VTC Spring)*, May 2016, pp. 1–5.
[27] L. You, K.-X. Li, J. Wang, X. Gao, X.-G. Xia, and B. Ottersten, "Massive MIMO transmission for LEO satellite communications," *IEEE J. Sel. Areas Commun.*, vol. 38, no. 8, pp. 1851–1865, Aug. 2020.
[28] S. K. S. Shin, K. L. Lim, K. C. Choi, and K. K. Kang, "Rain attenuation and Doppler shift compensation for satellite communications," *ETRI J.*, vol. 24, no. 1, pp. 31–42, Feb. 2002.
[29] J. Li, Y. Zhang, Y. Zhang, W. Xiong, Y. Huang, and Z. Wang, "Fast tracking Doppler compensation for OFDM-based LEO satellite data transmission," in *Proc. 2nd IEEE Int. Conf. Comput. Commun. (ICCC)*, Oct. 2016, pp. 1814–1817.
[30] U. Naeem, Z. Jawaid, and S. Sadruddin, "Doppler shift compensation techniques for LEO satellite on-board receivers," in *Proc. 9th Int. Bhurban Conf. Appl. Sci. Technol. (IBCAST)*, Islamabad, Pakistan, Jan. 2012, pp. 391–393.
[31] A. Abdi, W. C. Lau, M. Alouini, and M. Kaveh, "A new simple model for land mobile satellite channels: First- and second-order statistics," *IEEE Trans. Wireless Commun.*, vol. 2, no. 3, pp. 519–528, May 2003.
[32] I. Gradshteyn and I. Ryzhik, *Table of Integrals, Series and Products*, 7th ed. San Diego, CA, USA: Academic, 2007.
[33] M. Lin, Z. Lin, W.-P. Zhu, and J.-B. Wang, "Joint beamforming for secure communication in cognitive satellite terrestrial networks," *IEEE J. Sel. Areas Commun.*, vol. 36, no. 5, pp. 1017–1029, May 2018.
[34] V. S. Adamchik and O. I. Marichev, "The algorithm for calculating integrals of hypergeometric type functions and its realization in REDUCE system," in *Proc. Int. Symp. Symbolic Algebr. Comput. (ISSAC)*, 1990, pp. 212–224.
[35] M. K. Arti and V. Jain, "Relay selection-based hybrid satellite-terrestrial communication systems," *IET Commun.*, vol. 11, no. 17, pp. 2566–2574, Nov. 2017.
[36] K. An, M. Lin, J. Ouyang, and W.-P. Zhu, "Secure transmission in cognitive satellite terrestrial networks," *IEEE J. Sel. Areas Commun.*, vol. 34, no. 11, pp. 3025–3037, Nov. 2016.
[37] A. Zappone, P. Cao, and E. A. Jorswieck, "Energy efficiency optimization in relay-assisted MIMO systems with perfect and statistical CSI," *IEEE Trans. Signal Process.*, vol. 62, no. 2, pp. 443–457, Jan. 2014.
[38] M. Handley, "Using ground relays for low-latency wide-area routing in megaconstellations," in *Proc. 18th ACM Workshop Hot Topics Netw.*, Nov. 2019, pp. 125–132.
[39] Y. Zhang, J. Ye, G. Pan, and M.-S. Alouini, "Secrecy outage analysis for satellite-terrestrial downlink transmissions," *IEEE Wireless Commun. Lett.*, vol. 9, no. 10, pp. 1643–1647, Oct. 2020.
[40] G. Pan, J. Ye, Y. Zhang, and M.-S. Alouini, "Performance analysis and optimization of cooperative satellite-aerial-terrestrial systems," *IEEE Trans. Wireless Commun.*, vol. 19, no. 10, pp. 6693–6707, Oct. 2020.

Jia Ye (Student Member, IEEE) was born in Chongqing, China. She received the B.Sc. degree in communication engineering from Southwest University, Chongqing, in 2018, and the M.S. degree from the King Abdullah University of Science and Technology (KAUST), Saudi Arabia, in 2020, where she is currently pursuing the Ph.D. degree. Her main research interest includes the performance analysis and modeling of wireless/wireless communication systems.

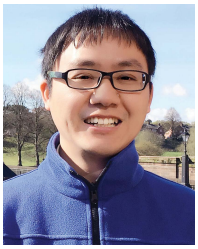

Gaofeng Pan (Senior Member, IEEE) received the B.Sc. degree in communication engineering from Zhengzhou University, Zhengzhou, China, in 2005, and the Ph.D. degree in communication and information systems from Southwest Jiaotong University, Chengdu, China, in 2011. Since November 2020, he has been with the School of Cyberspace Science and Technology, Beijing Institute of Technology, China, as a Professor. His research interests include communications theory and signal processing.

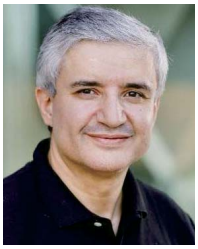

Mohamed-Slim Alouini (Fellow, IEEE) was born in Tunis, Tunisia. He received the Ph.D. degree in electrical engineering from the California Institute of Technology (Caltech), Pasadena, CA, USA, in 1998. He served as a Faculty Member with the University of Minnesota, Minneapolis, MN, USA, and the Education City, Texas A&M University at Qatar, Doha, Qatar, before joining the King Abdullah University of Science and Technology (KAUST), Thuwal, Saudi Arabia, as a Professor of electrical engineering, in 2009. His current research interests include the modeling, design, and performance analysis of wireless communication systems.